NAS 7-49(04)

9990-6420-RU-000

24p.

N63 18415

CODE-1

UNPUBLISHED PRELIMINARY DATA

FEASIBILITY OF REMOTE COMPOSITIONAL MAPPING OF THE LUNAR SURFACE

Effects of Surface Roughness

23 May 1963

by

Eugene A. Burns

Space Technology Laboratories, Inc.
Redondo Beach, California

and

R. J. P. Lyon

Stanford Research Institute
Menlo Park, California

8298002

OTS PRICE

XEROX $ 2.60 ph

MICROFILM $ 0.92 mf.

CR-50,544

ABSTRACT

18415

Spectra obtained by total infrared reflectance measurements for rock and mineral powders with varying degrees of surface roughness has permitted calculations of realistic spectral emissivity curves for these materials. Although the amplitude of the observed deviations from a black-body in the 8 to 12μ region are not as large as that reported previously for polished surfaces, diagnostic differentiation between acid (granite) and basic (dunite, or meteorite) rock type powders in a size less than 100μ is clearly feasible. Total reflection measurements of alumina and quartz together with direct emission measurements of quartz in various surface conditions show diminishing detail as the particle size is reduced. By suitable calibration it would be possible to obtain information concerning the lunar surface aggregate characteristics by remote sensing.

Consideration of an instrument capable of remote compositional mapping of the lunar surface by measurement of the diagnostic spectral emissivity curves results in the recommendation of a modified Perkin-Elmer Model SG-4 Spectrophotometer. A discussion of the constraints imposed on the design of this instrument for spectral resolution, weight, signal-to-noise ratio, detector temperature and configuration, and power requirements is presented together with the implications of these factors on the objectives of compositional mapping from a spacecraft.

INTRODUCTION

Reflected infrared spectral analysis has been shown to characterize the composition of geological assemblages (1). Recently, well-defined infrared reflectance spectra have been obtained for mineral and rock types suspected to exist on the moon (2). These measurements were obtained for minerals having polished surfaces. Since it is believed that lunar surface, at least in part, consists of particulate matter, it is necessary to extend the infrared spectral data to cover a range of possible lunar aggregate forms. Such data will permit an early assessment of the types of information most readily attainable from remote spacecraft exploration. To implement remote measurements of lunar surface properties during planned satellite missions, consideration should be given at this time to adapting current infrared equipment and techniqes. The development of lightweight remote sensing devices utilizing available missile power appears to be feasible (3). However, systems analysis and consideration of additional instrument design are necessary to define the specific lunar mission.

This paper presents information pertinent to two technical areas associated with a successful study of the lunar surface from a remote satellite. The first part of the paper discusses the spectral response of lunar materials of varying surface properties, whereas the second part describes the instrumentation design constraints and practicability with regard to satellite mission considerations.

BACKGROUND DISCUSSION

It is well established that the thermal emission spectral characteristics of materials can be predicted from knowledge of intermolecular vibrations of molecules present on the surface of the material (4, 5). We have developed the utilization of this phenomenon for qualitative identification of geological surface composition(1). It is reasonable, therefore, to believe that the surface of the moon can be identified by measurement of its thermal radiation as a function of wavelength provided that the surface has a suitable physical form. The classic 1930 and 1940 interpretations by Pettit and Nicholson (6, 7) from which they contend the moon is a black body have recently been shown to be in error (8, 9). At this time the precise thermal emission characteristics of the moon have not yet been identified, primarily because of the 9 to 10μ infrared absorption by ozone in the earth's atmosphere.

Our scientific thesis is: The spectral emissivity curve, $\epsilon(\lambda)$, (variations in the emissivity as a function of wavelength) can serve as a diagnostic fingerprint of a particular geological assemblage. In the past we have proven this thesis qualitatively from transmission measurements (10) and quantitatively from reflection measurements of various rock and mineral compositions (2, 9). In the literature there is

controversy with respect to the effect of particle size and surface roughness on emissivity. It has been observed that emissivity is independent of particle size (11), whereas others have found that emissivity increases as the surface is roughened; it is seriously affected by porosity, and depends on material geometry and surface state (12, 13). Because the validity of our scientific thesis for compositional mapping is dependent on observing deviations from black body characteristics for lunar surface materials in various states of aggregation, we have undertaken a study of the spectral emissivity as a function of particle size.

EXPERIMENTAL CONSIDERATIONS AND RESULTS

Experimental difficulties limit the use of emission measurements, hence in the past we have evaluated $\epsilon(\lambda)$ indirectly by use of Kirchhoff's law permitting the conversion of reflectance data to emission data. From Fig. 1 it is seen that the radiant energy incident on a substrate can be reflected, scattered, absorbed, or transmitted, i.e.,

$$I_o = I_\rho + \Sigma I_s + I_\alpha + I_t. \quad (1)$$

This is true for any wavelength, hence upon division by the incident energy,

$$1 = \rho(\lambda) + s(\lambda) + \alpha(\lambda) + t(\lambda), \quad (2)$$

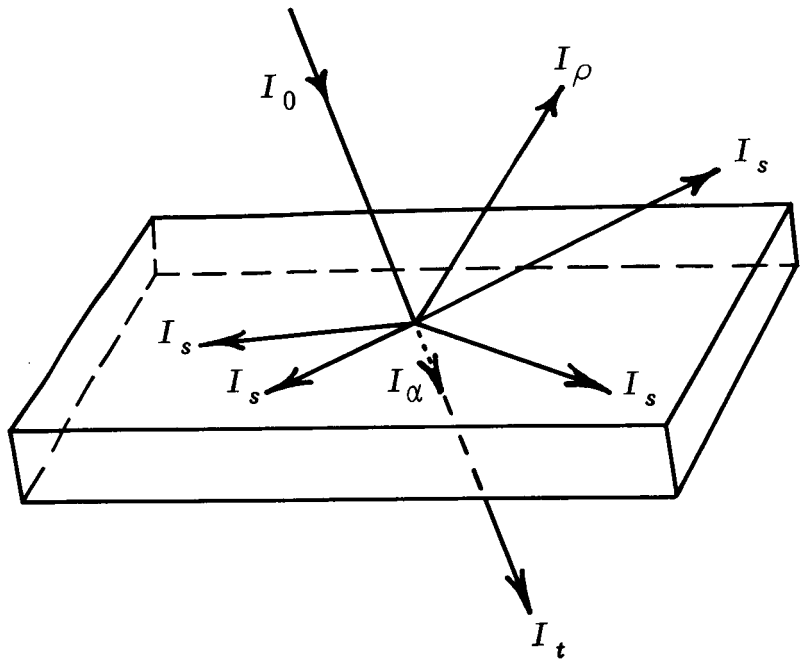

Fig. 1 Kirchhoff's Law: $I_o = I_p + \lesssim I_s + I_\alpha + I_t$

where $\rho(\lambda)$, $s(\lambda)$, $\alpha(\lambda)$, and $t(\lambda)$ are respectively the reflectivity, scattering coefficient, absorptivity, and transmittancy as a function of wavelength. At thermal equilibrium, the energy absorbed must be equal to that radiated, or

$$\epsilon(\lambda) = 1 - \rho(\lambda) - s(\lambda) - t(\lambda). \qquad (3)$$

It follows, for opaque, polished materials where $t(\lambda)$ and $s(\lambda) = 0$, $\epsilon(\lambda)$ can readily be obtained from $\rho(\lambda)$. Because it is not clear from the literature whether emissivity is independent of surface properties of the material, the emissivity-surface property relationship needs assessment for its applicability to lunar measurements.

By measurement of the integrated reflectance, including the scattered components, it is possible to determine $\epsilon(\lambda)$ experimentally for powdery substances. The experimental set-up employed is that developed by J. T. Bevans (14) and is shown in Figs. 2 and 3. This apparatus incorporates a black-body source with a temperature range of 500 to 2000°F, two 7-1/2 degree off-axis paraboloid front-surface mirrors, temperature controlled sample holder, and a Perkin Elmer Model 13C infrared monochrometer and detector. For this work, the powders were compacted into a sample cup which permitted examination at a vertical sample inclination. The mirrors and sample holder were maintained at ambient temperature by conduction with circulated cooling water throughout the measurements.

The spectral emissivity curves obtained using this apparatus and Eq. 3 are shown in Fig. 4. These curves clearly indicate that differentiation of acid and basic type rocks, granite and dunite, is possible in the particle size range of 100μ As might be expected, some of the fine structure seen with polished specimens is obliterated, or less definite, in the spectra of powdered samples; however, the diagnostic use of the spectral emissivity curve is demonstrated.

The effect of particle size on the calculated emissivity curves for alumina is shown in Fig. 5. As the particle size of alumina goes down from sapphire, polycrystalline platelets, coarse-grained material,"to a 2μ* powder,"the calculated emissivity curve approaches a black-body curve. In fact,"2μ"alumina is almost a perfect black body in the wavelength range 8μ to 25μ. Similar studies of quartz, shown in Fig. 6, reveal the same generalities:

* Subsequent electromicroscope studies revealed this to have a mean particle size of about 200 angstroms (0.02 microns)

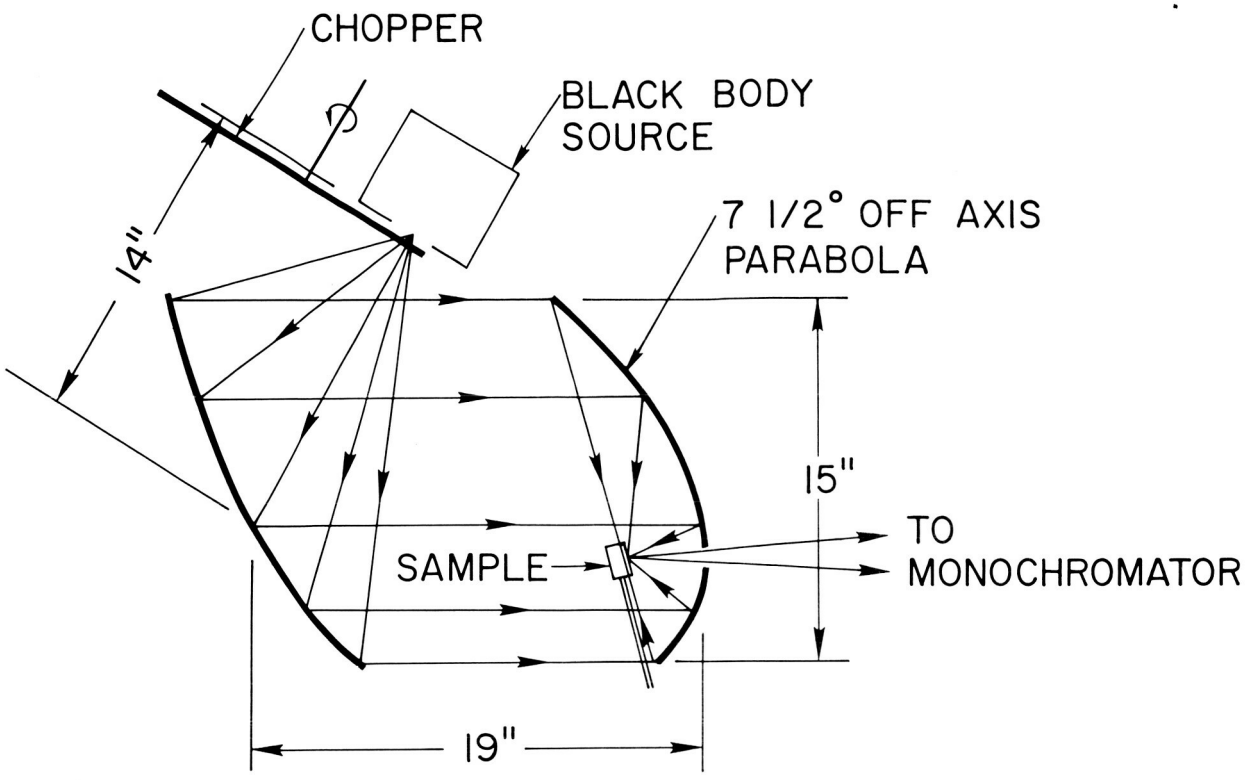

Fig. 2 Optical Configuration of Parabaloid Reflectometer

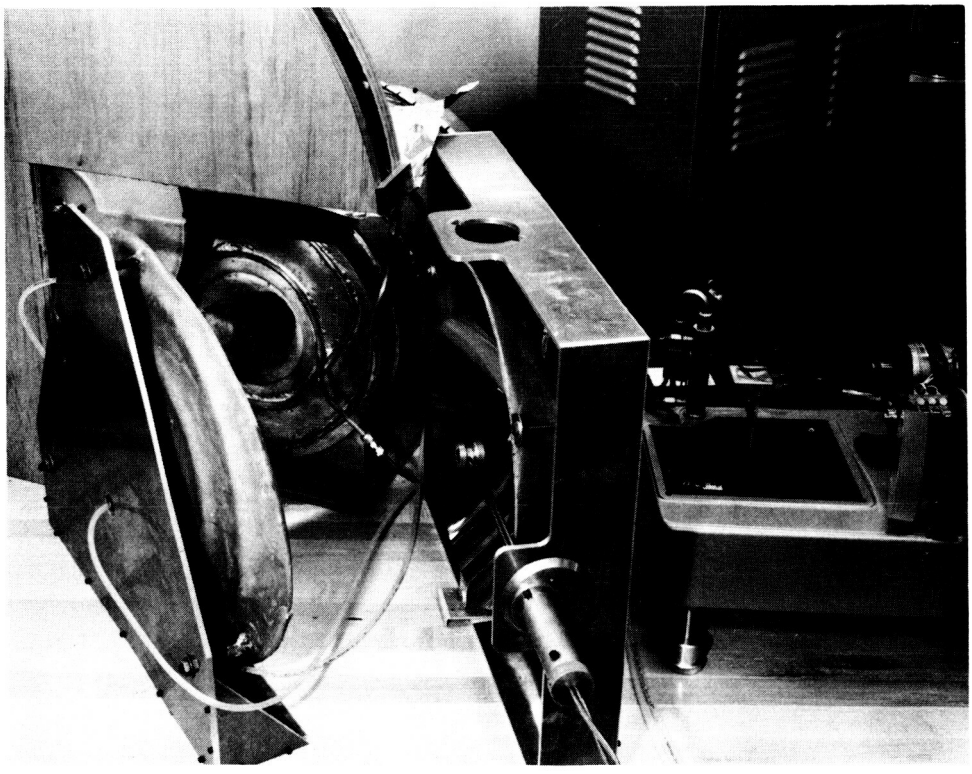

Fig. 3 STL-Developed Paraboloid Reflectometer

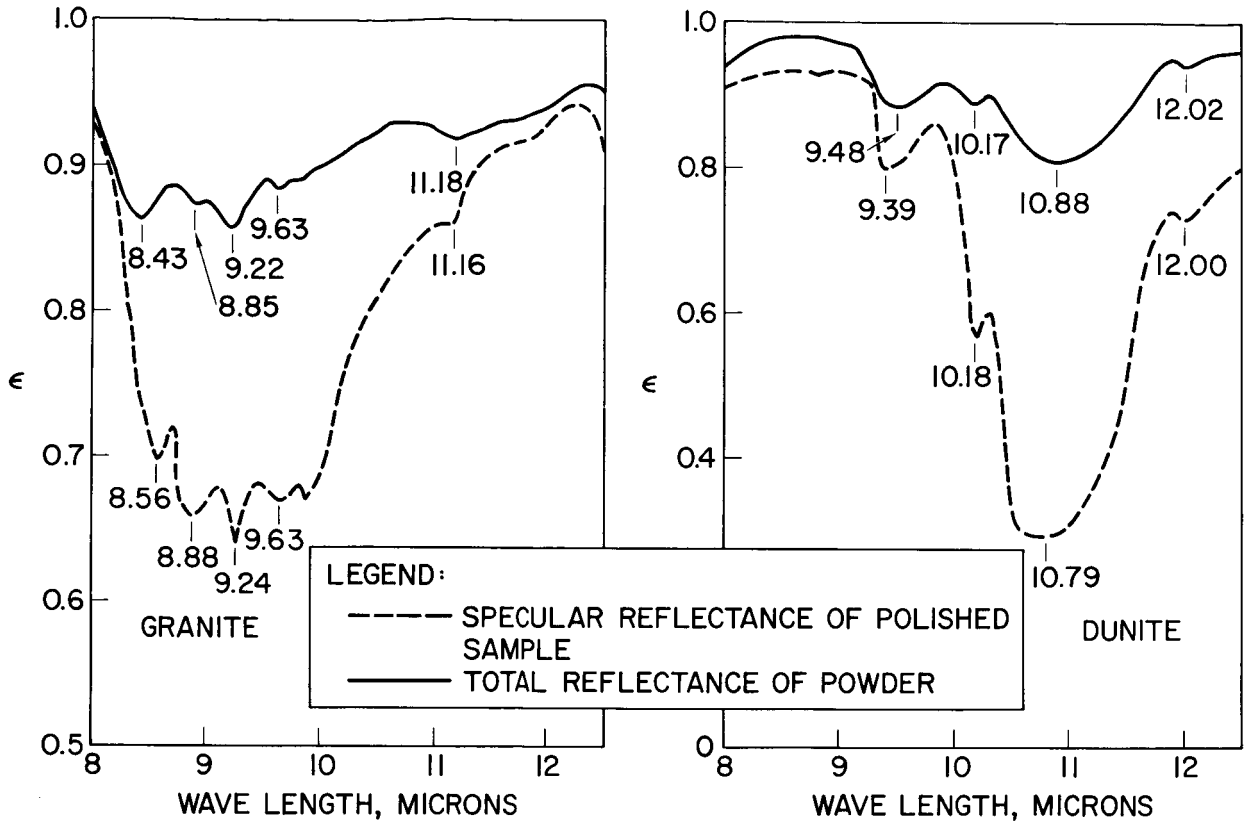

Fig. 4 Calculated Emissivity Curves for Dunite and Granite - Polished Plates and 100μ Powder

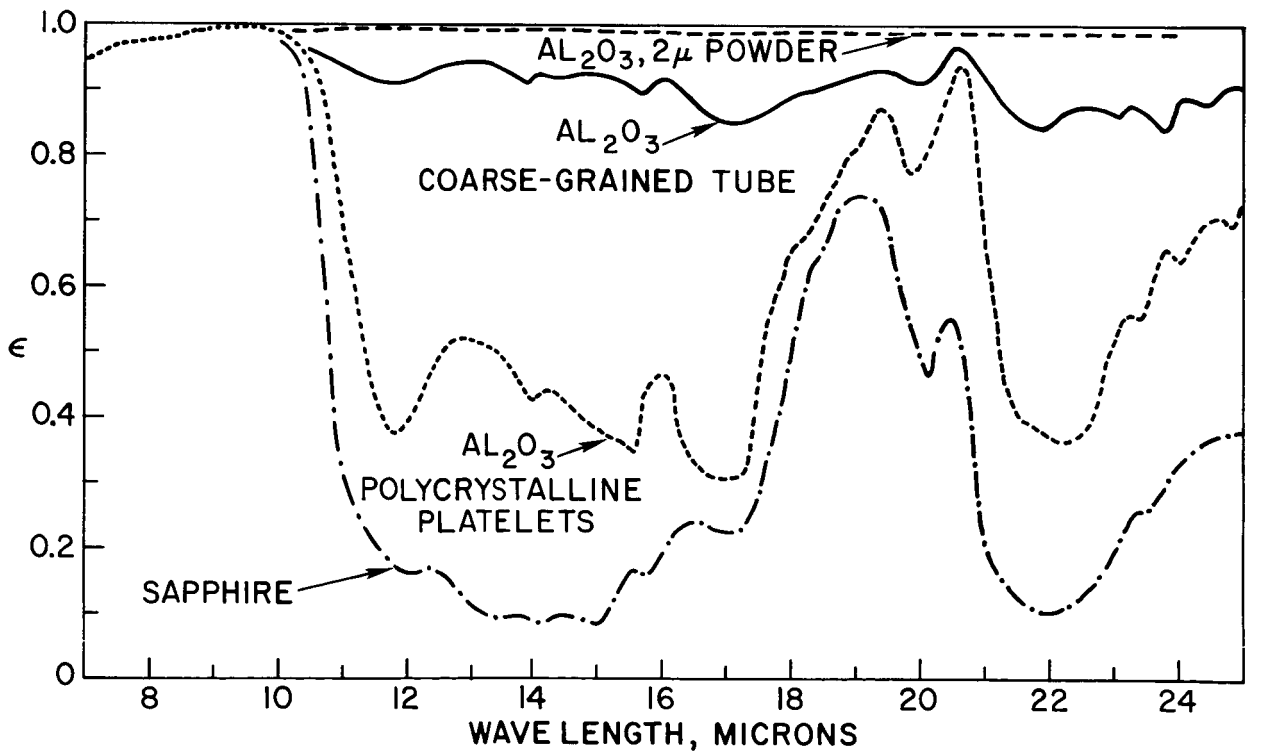

Fig. 5 Calculated Emissivity Curves for Alumina in Various Surface Aggregations

detail of the quartz restrahlen is evident at a -325 mesh size (44μ); however, some of the fine structure evident for a polished quartz X-cut plate and 400μ quartz sand is missing.

As mentioned above, direct emission measurements possess experimental difficulties, such as sample temperature control -- both absolute control and homogeneity in the source, stray emission from heated mirrors, and energy absorption by the monochrometer. In spite of these difficulties, we have initiated some emission experiments to test the diagnostic utility of this method, for as it is proposed, the emission measurement is what will be obtained in actual compositional mapping. Instead of transmitting through the two filters to a detector, the radiant energy was collimated into a Perkin-Elmer Model 112 Double Pass Infrared Spectrometer, and the sample emission was recorded as a function of wavelength.

Emission data for solid quartz, K-feldspar, and dunite appear in Fig. 7. Preliminary emission data for quartz in various particle sizes is shown in Fig. 8. Quartz, with a very dominant restrahlen at 9.05μ shows structure even at a particle size of 1 to 2μ; however, its wavelength location is shifted to slightly higher wavelengths. For these data the sample was maintained at about 520°K, and the full-scale response was 1μV.

The experimental results show that diagnostic differention between various rock types is feasible provided the surface of the moon is not covered with a dust with particle size less than about 10μ. Further, by establishing the precise relationship of $\epsilon(\lambda)$ with particle size, it appears possible to make some estimates of the general particle size characteristics of the lunar surface.

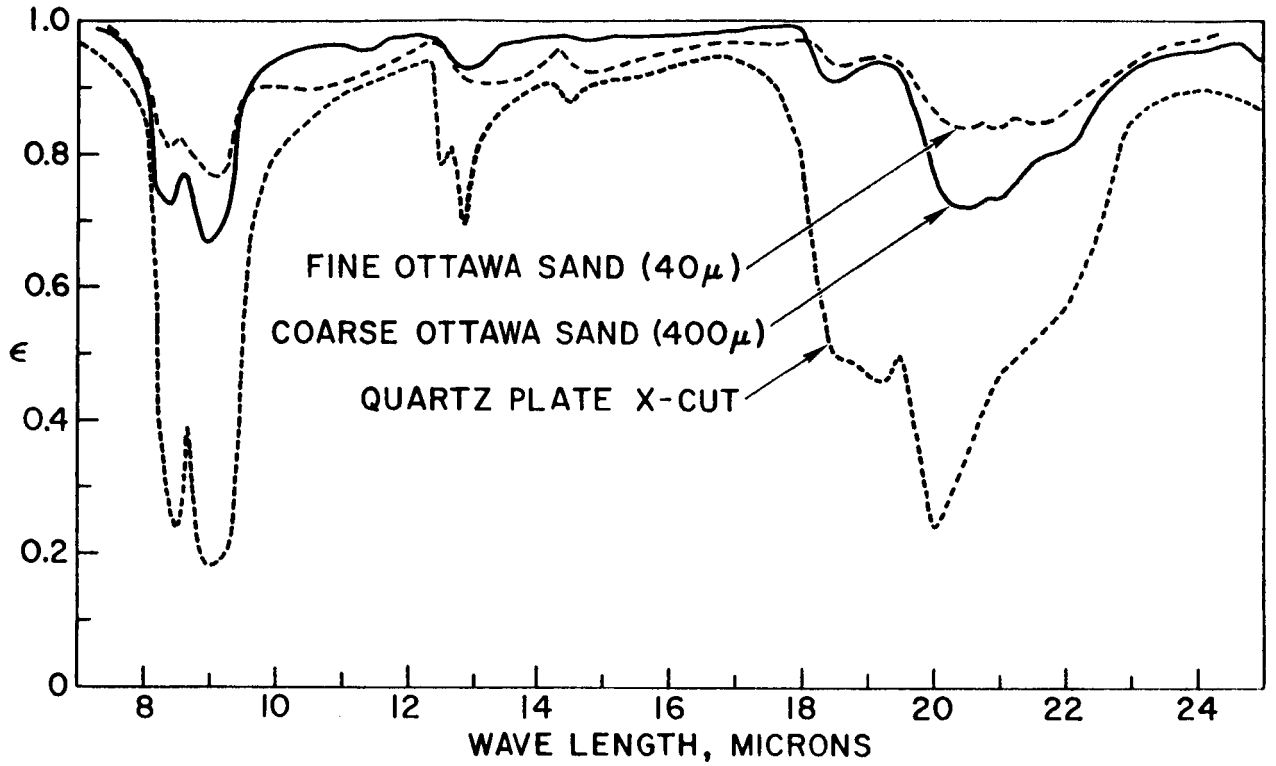

Fig. 6 Calculated Emissivity Curves
for Quartz in Various Surface Aggregations

Fig. 7

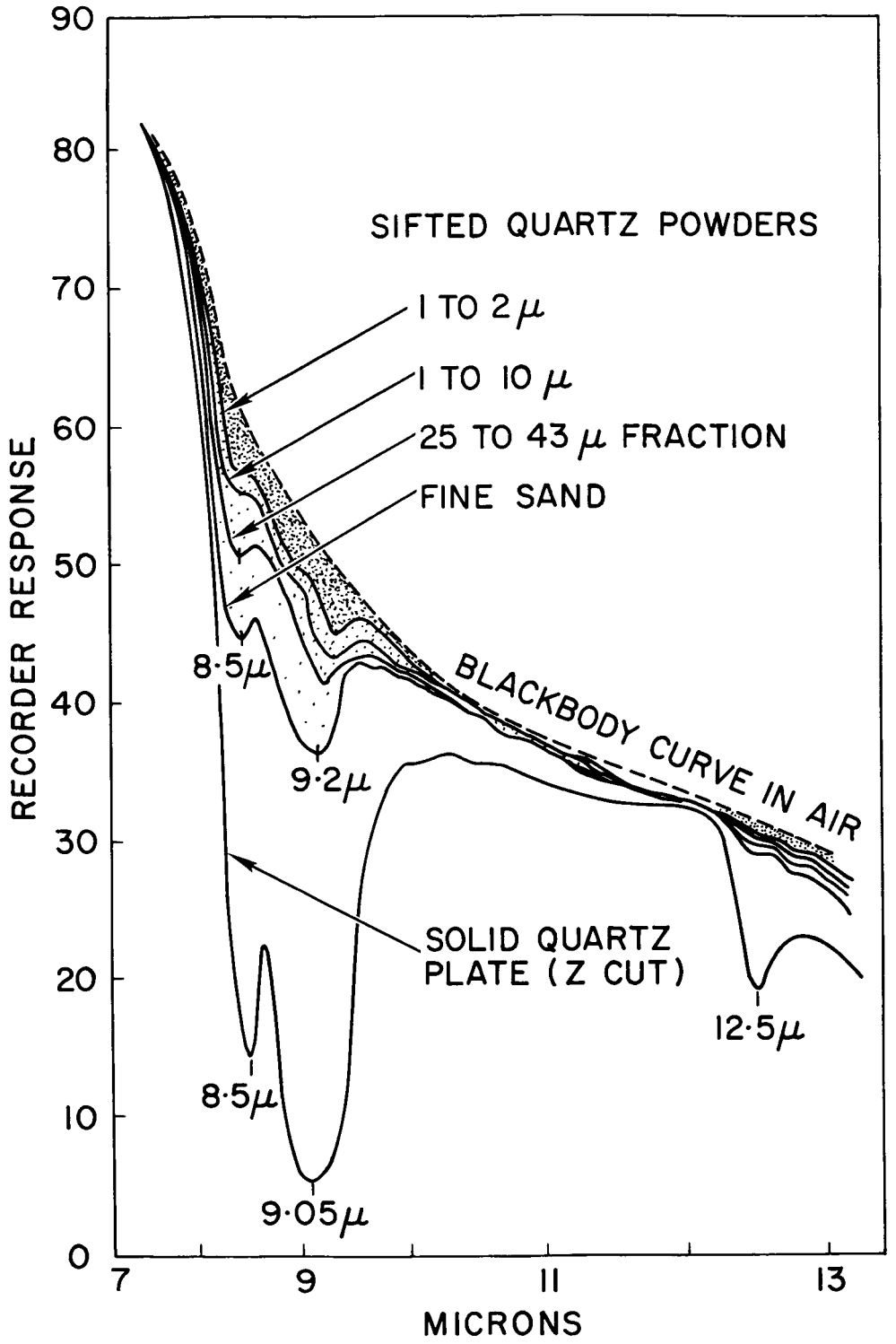

Fig. 8 Emission Curves for Quartz in Various Surface Aggregations

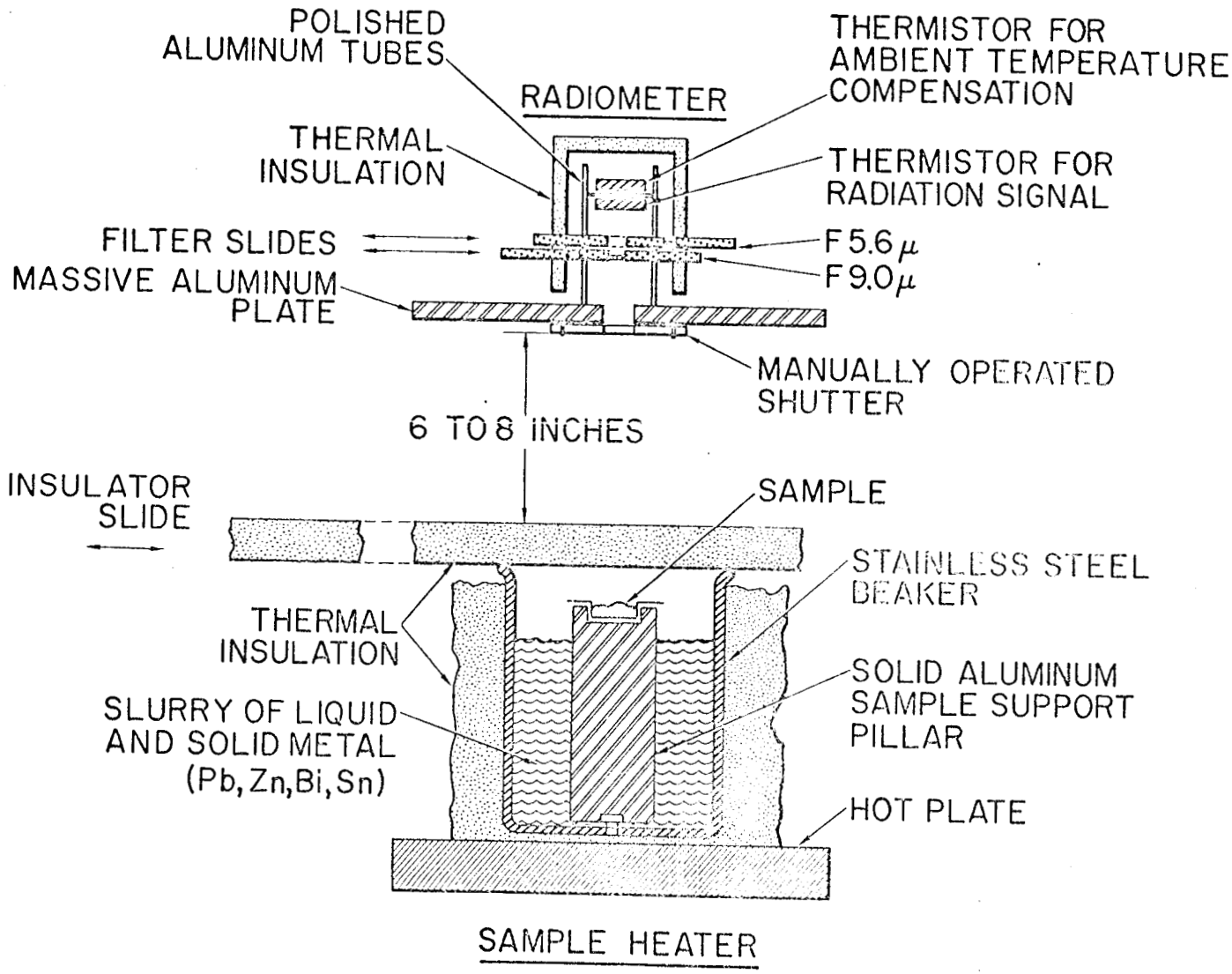

FIG. 7 EXPERIMENTAL RADIOMETER FOR STUDYING FINE-GRAINED MATERIALS

INSTRUMENTATION FOR LUNAR COMPOSITIONAL MAPPING

For implementation of the lunar compositional mapping, several approaches to the instrumentation with spacecraft constraints of simplicity, low weight, good resolution, high signal-to-noise ratio, and low power requirement were considered. Ideally, it is desirable to obtain the spectral response for a specific location; however, due to difficulties in obtaining a multitude of matched detectors for every desired wavelength, and the lag in the development of photographic detectors suitable for this purpose, it has been expeditious to consider an instrument which will scan wavelength. Because the spacecraft is in motion, the areal view at the start of the scan is not the same as that at the end of the scan. In Fig. 9 the trajectories of two orbits -- one a circular orbit of about 100 miles from the surface and one an elliptical orbit with a perigee of 25 miles and apogee of 1000 miles -- are shown together with the area subtended by an instrument with a field of view of 2.4×10^{-4} steradians, or an angle of 1°, with a scanning rate of 20 seconds. These orbits were chosen as typical of those to be utilized in the NASA-sponsored lunar photography experiment (15). A general expression for the areal coverage from this type of experiment is

$$A = \frac{2 h_p s r_m^2}{r_m + h_p} \sqrt{\frac{g_m \Omega (1+e)}{\pi (r_m + h_p)}} + h_p^2 \Omega \qquad (4)$$

where h_p is the altitude of the spacecraft at perigee, s is the spectral scan period, r_m is the radius of the moon, g_m is the gravity of the moon, Ω is the solid angle subtented by the instrument, and e is the eccentricity of the elliptical orbit, [$e = (h_a - h_p)/(2r_m + r_p + h_a)$; $e = 0$ for a circle; at the apogee, when h_a supplants h_p, the term $(1+e)$ becomes $(1-e)$] . The resulting shape is a long rectangle with rounded ends; the length of these strips is dependent on the spectral scanning rate.

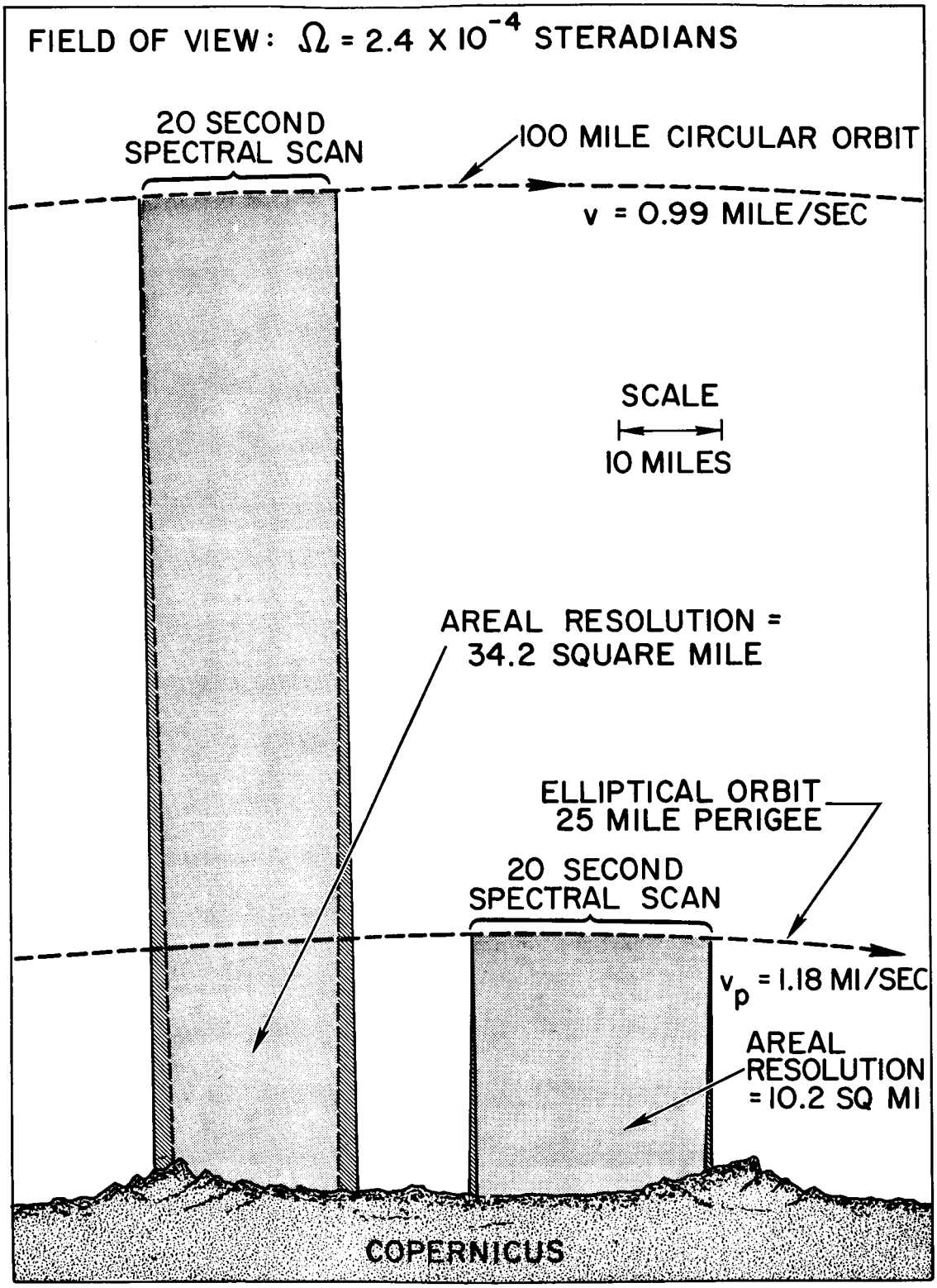

Fig. 9 Field of View from Two Defined Orbits at a 20 sec Scanning Period

For a fixed Ω and orbit (h_p), the scan rate is the major variable to be changed to improve the areal resolution. However, tradeoffs are required here; namely, as the scan rate is increased, the detector can not respond to small change in the spectra, the instrument lags, and fine detailed spectra are not obtained, i.e., optical resolution is reduced. In a similar fashion, reducing the view angle reduces the energy observed by the instrument, thus reducing the signal-to-noise ratio. Lowering the altitude improves the areal resolution without reducing the energy available for the instrument.

It would be possible to install the spectrometer on a gimballing mount to focus on a single location; however, in the interest of simplicity this concept was abandoned. One can readily see the difficulties associated with altitude variations.

The signal-to-noise ratio obtainable is a critical consideration, particularly if diagnostic information at higher wavelengths (i.e., 20μ is to be obtained. To improve this ratio, new sensitive infrared detectors (16) must be employed; however, they require cooling to liquid neon or helium temperature, which introduces further complications. Use of liquid helium stored in a reasonable size dewar precludes a mission in which useful information can be obtained beyond 5 days. This is not too much of a problem for a moon orbiter, for with only a three-day journey two days of information could be obtained. (26 lunar orbits -- over 8500 spectral scans). A recent advance in the state-of-the-art has produced a lightweight cryostat with a low power requirement indicating this technique may permit long duration experiments (17). With these considerations in mind, we have recommended the incorporation and modification of the Perkin-Elmer Model SG-4 Soectrophotometer shown in Fig. 10 for this type of

mission (3). This instrument weighs less than 30 lbs. including its electronic control feedback circuitry, and requires 10 watts power. Discussions with Perkin-Elmer Corp. indicate the weight of this instrument can be reduced significantly. The optical set-up of the instrument is seen schematically in Fig. 11. Use of Cassegrainian telescopic optics permits a large collector surface with an increased focal length. The electrical controls block diagram for the instrument is seen in Fig. 12. Use of the two-channel output, one showing grating orientation as a function of time and the other showing detector output as a function of time, permits the calculation of output vs. wavelength curve. An example of the response typically obtained from this instrument in the 2 to 4μ region is seen in Fig. 13. The grating would be changed to operate between 7 and 14μ for the compositional mapping mission. The signal-to-noise ratio obtainable for this instrument is calculated from the following expression:

$$\left(\frac{S}{N}\right)_{\lambda,T} = \frac{ED^{*}A_c \curvearrowleft t\Delta\lambda}{\pi^2 \ell \sqrt{2 f_0 A_0}} W_0(\lambda,T) \qquad (5)$$

Where E = is the optical efficiency of the system = 0.80 (reflectivity of six surfaces) x 0.45 (grating efficiency) x 0.60 (filter transmission) x 0.90 (detector efficiency) = 0.195

D^{*} = the detector detectivity at a specific wave length and temperature

A_c = area of the Cassegrainian collecting system (6.0 inch diameter less 2.3 inch diameter reflecting surface) = 155 cm^2

$\curvearrowleft$ = field of view = 2.4×10^{-4} steradians

t = slit width = 0.1 cm

$\Delta\lambda$ = spectral resolution = 0.054μ

Fig. 10 Perkin-Elmer Model SG-4 Spectrophotometer

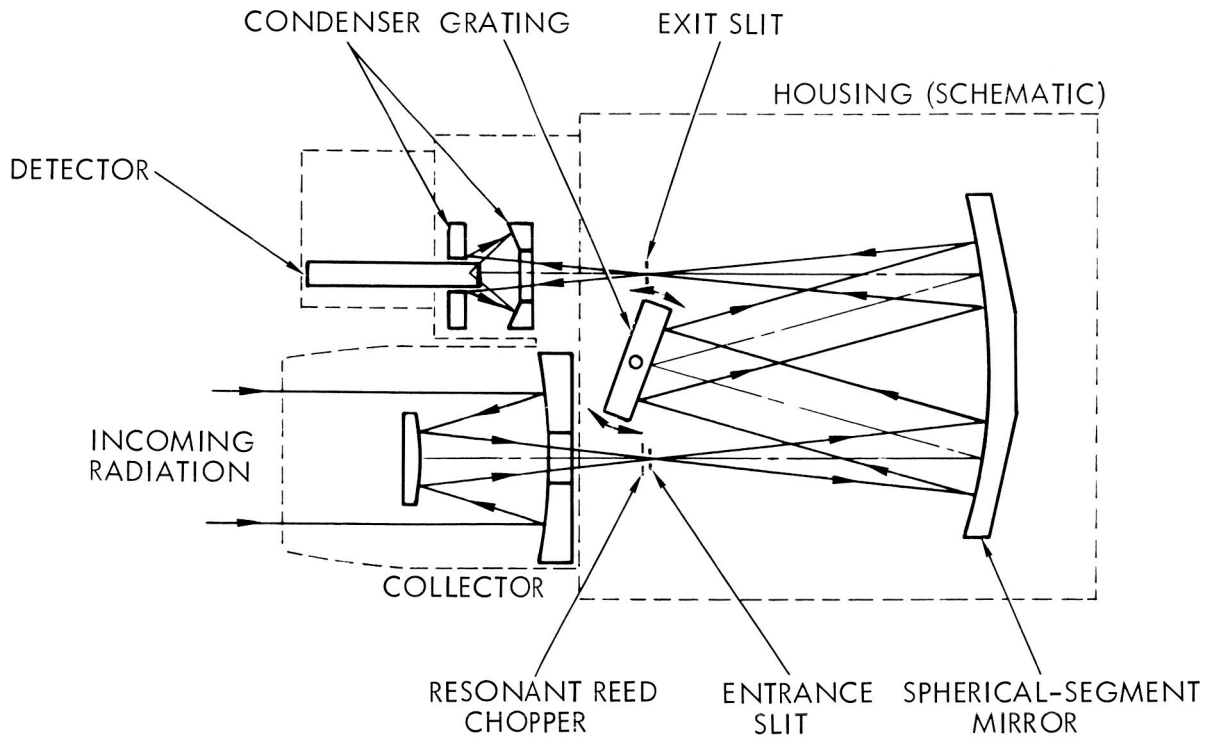

Fig. 11 Schematic Diagram of SG-4 Optical System

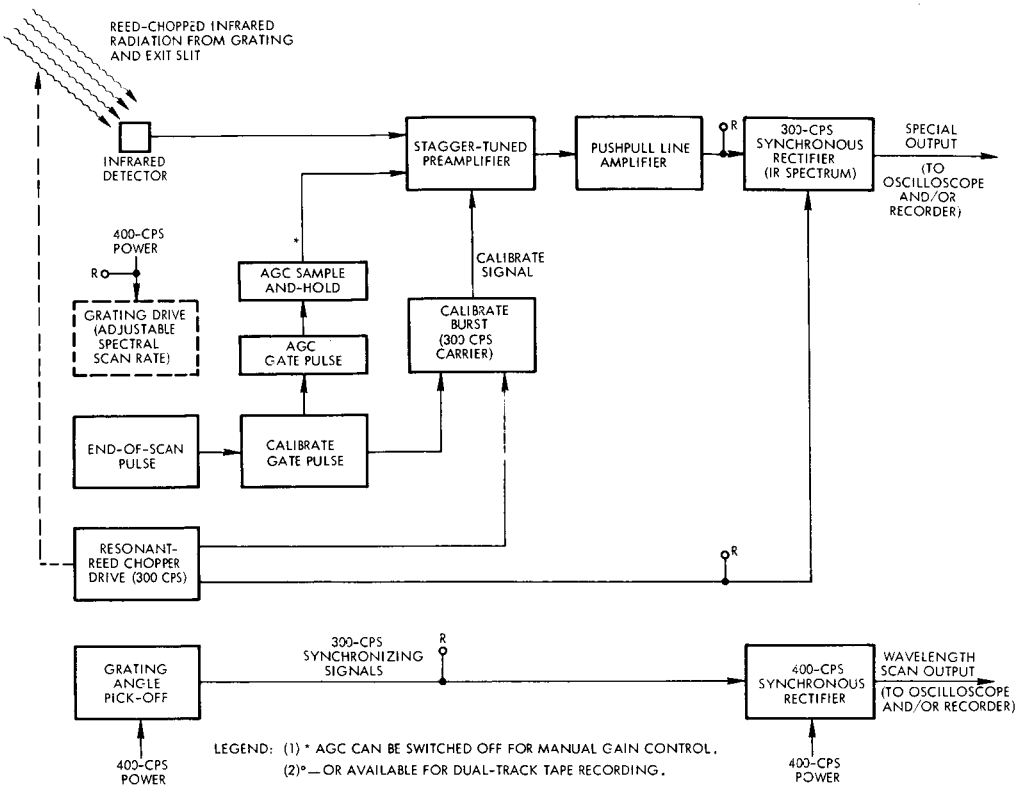

Fig. 12 Electronics Block Diagram of Perkin-Elmer SG-4

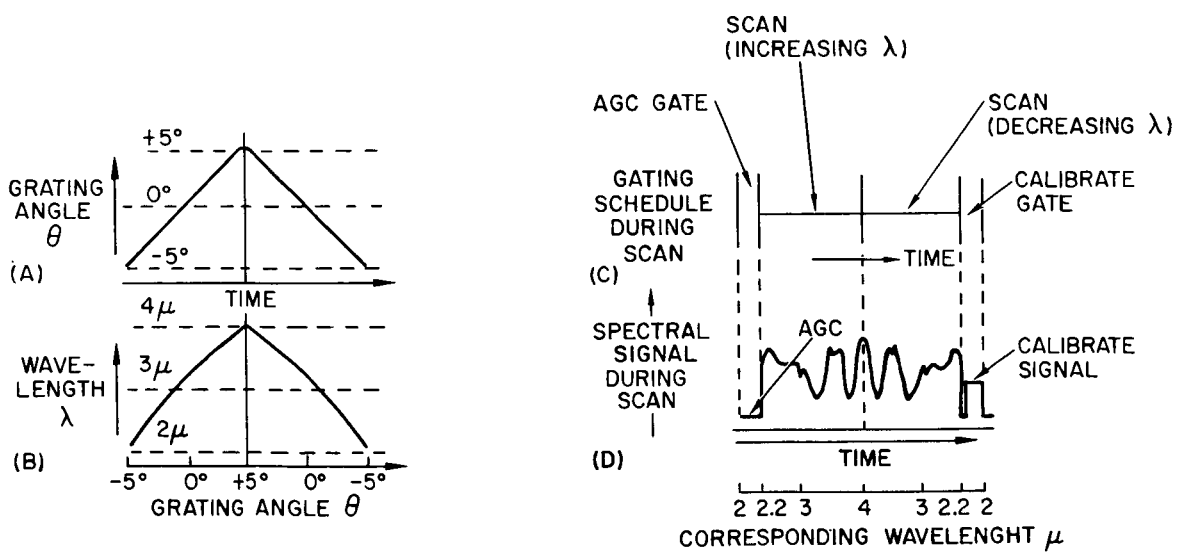

Fig. 13 Functional Plots and Wave Forms

$W_o(\lambda,T)$ = energy flux available from lunar surface

ℓ = slit height = 0.6 cm

f_o = modulating carrier frequency = 300 cps

A_o = area of detector = 5.5×10^{-4} cm^2

For a lunar surface temperature of 350° K and at a wave length of 10μ using a cadmium-doped germanium detector at 25° K, $W_o(\lambda,t) = 2.0 \times 10^{-3}$ watt/cm^2 - μ - ster and $D^* = 1.6 \times 10^{10}$ cm-$cps^{1/2}$/$watt_{rms}$ [NEP = 1.2 p watt/$cps^{1/2}$], hence S/N = 342. At a wave length of 20μ, $W_o(\lambda,t)$ = 5.5×10^{-4} watt/cm^2-μ-ster, and the same detector has $D^* = 3.6 \times 10^{10}$ cm - $cps^{1/2}$/$watt_{rms}$ [NEP = 0.65 p watt/$cps^{1/2}$], hence S/N = 210. These calculations indicate that there is sufficient energy available to permit detection and measurement of the deviations from black body behavior.

20

CONCLUSIONS AND RECOMMENDED APPROACH

From the work presented here, we conclude that remote infrared spectral measurement of the lunar surface will provide valuable information for geological compositional mapping and may also introduce a method to determine its general particulate structure. If the average particle size of the Maria is less than about 10μ, infrared spectral emission sensing is an excellent technique for accurate temperature mapping. If areas of the moon consist of a surface having a coarse structure (bare rocks free of dust, such as those recently broken by meteroite impact, or cliffs too steep to hold a dust layer), we are confident that compositional mapping of these areas can be conducted. The information from these remote measurements is best when accomplished from an orbiting satellite, because complete lunar mapping is possible at maximum areal resolution.

Some highly meaningful results can also be obtained by measurements from a high altitude balloon; namely, 1) distinction of the "basic" rock types in the lunar surface (i.e., meteorite, dunite, gabbro, etc.) and 2) precise measurement of the ozone concentration as a function of altitude. Measurements from a high-altitude balloon could be performed sooner since instrumental development time is minimal at a cost lower than that required for a lunar spacecraft mission.

ACKNOWLEDGEMENT

The authors wish to acknowledge the National Aeronautics and Space Administration for financial support for that portion of the work conducted at the Stanford Research Institute.

REFERENCES

1. Lyon, R. J. P. and Burns, E. A., "Analysis of Rocks and Minerals by Reflected Infrared Radiation," Econ. Geol. 58, 274 (1963)

2. Lyon, R. J. P. and Burns, E. A. "Infrared Spectral Analysis of the Lunar Surface from an Orbiting Spacecraft," Proceedings of the Second Symposium on Remote Sensing of Environment, held October 15-17, 1962, University of Michigan, February 1963, pgs 309-327.

3. Sachs, H., Perkin-Elmer Corporation, Private Communication, March 8, 1963.

4. Coblenz, W. W., "Investigation of Infrared Spectra," Carnegie Institution of Washington, 1906.

5. McMahon, H. O., "Thermal Radiation Characteristics of some Glasses," Journal of American Cer. Society., 34, 91 (1951).

6. Pettit, E., and Nicholson, S. B., "Lunar Radiation and Temperature," Astrophysics Journal, 71, 102 (1930).

7. Pettit, E., "Radiation Measurements of the Eclipsed Moon," Astrophysics Journal 91, 408 (1940).

8. Burns, E. A., and Lyon, R. J. P., "Errors in the Measurement of the Temperature of the Moon," Nature 196, 463 (1962).

9. Burns, E. A., and Lyon, R. J. P., "Errors in the Measurement of the Lunar Temperature," Astrophysics Journal, In Press.

10. Lyon, R. J. P., "Evaluation of Infrared Spectrophotometry for Compositional Analysis of Lunar and Planetary Soils," Final Report SRI Project SU-3943, NASA Contract NASr-49(04), September 1962.

11. Sully, A. H., Brandes, E. A., and Waterhouse, R. B., "Some Measurements of the Total Emissivity of Metals and Pure Refractory Oxides and the Variation of Emissivity with Temperature," Brit. J. APP.Phys. 3, 97 (1952).

12. Crowley, D. E., "Emittance and Reflectance in the Infrared. An annotated Bibliography," Report No. 2389-15-5, University of Michigan, Willow Run Laboratories, Ann Arbor, Michigan, April 1959, p. 140.

13. Blau, H. H., Miles, J. H., and Ashman, L. E., "The Thermal Radiation Characteristics of Solid Materials," Air Force Cambridge Research Center AFCRC TN-58-132, March 31, 1958, p. 9.

14. Bevans, J. T., Private Communication, 1962.

15. "A Lunar Photographic Mission in 1964," Space Technology Laboratories, Inc. Redondo Beach, California, March 1963.

16. Wolfe, W. L., and Limperio, T., "Quantum Point Detectors," Space/Astronautics, November, 108, (1961).

17. Otani, H., "A Miniature Single-Stage Cryogenerator for Cooling Down to 30 Degrees Kelvin, "Norelco Reporter 9, 56 (1962).

STANFORD RESEARCH INSTITUTE

MENLO PARK
CALIFORNIA

Regional Offices and Laboratories

Southern California Laboratories
820 Mission Street
South Pasadena, California

Washington Office
808 17th Street, N.W.
Washington 5, D.C.

New York Office
270 Park Avenue, Room 1770
New York 17, New York

Detroit Office
The Stevens Building
1025 East Maple Road
Birmingham, Michigan

European Office
Pelikanstrasse 37
Zurich 1, Switzerland

Representatives

Honolulu, Hawaii
Finance Factors Building
195 South King Street
Honolulu, Hawaii

London, Ontario, Canada
85 Wychwood Park
London 14, Ontario, Canada

London, England
15 Abbotsbury Close
London W. 14, England

Milan, Italy
Via Macedonio Melloni 40
Milano, Italy

Tokyo, Japan
911 Iino Building
22, 2-chome, Uchisaiwai-cho, Chiyoda-ku
Tokyo, Japan